Generalized Binet Dynamics

Chen Ning

Faculty of Information & Control Engineering, Shenyang Jianzhu University,
Shenyang, China, 110168
e-mail: n_chen@126.com

Clifford A. Reiter

Department of Mathematics, Lafayette College, Easton, PA 18042 USA
e-mail: reiterc@lafayette.edu

Abstract

The Binet formula provides a mechanism for the Fibonacci numbers to be viewed as a function of a complex variable. The Binet formula may be generalized by using other bases and multiplicative parameters that also give functions of a complex variable. Thus, filled-in Julia sets that exhibit escape time may be constructed. Moreover, these functions have computable critical points and hence we can create escape time images of the critical point based upon the underlying multiplicative parameter. Like the classic Mandelbrot set, these parameter space images give a type of atlas into the Julia sets.

Keywords: Complex dynamics, critical point dynamics, M-set, Julia Set, generalized Binet formula

1. Introduction

The Fibonacci numbers are given by the sequence 0, 1, 1, 2, 3, 5, 8, 13, ... where each term is the sum of the previous two. This sequence can be defined via the recursive formulas: $F_0 = 0$, $F_1 = 1$, and $F_n = F_{n-1} + F_{n-2}$. However, we can also use the well known

Binet formula [1-3] which may be described as follows. Let $\tau = \dfrac{1 + \sqrt{5}}{2} \approx 1.618$ and

$\bar{\tau} = \dfrac{1 - \sqrt{5}}{2} \approx$ -0.618 where τ is the golden ratio and $\bar{\tau}$ is the algebraic conjugate of τ.

Then the Binet formula, $F(z) = \dfrac{\tau^z - \bar{\tau}^z}{\sqrt{5}}$, is a complex function that is a generalization

of the Fibonacci sequence. However, because this function involves the negative base $\bar{\tau}$, it takes complex values along the real line. Thus, while it gives a generalization to the complex domain, it does not give a generalization to the real domain.

In [4], the escape time of $F(z)$ was examined, and an interesting spiral around the origin was observed. This investigation is the final step in a natural progression of investigations that began with that observation of a spiral; that was followed by considering functions with a multiplicative parameter that made the spiral more dramatic. Those functions were then considered with a generalized base. Then, realizing that the critical points could be computed, we were ready to study the dynamics of the critical points. Thus, in this investigation we study the dynamics of functions similar to the function $F(z)$ that was studied in [4], but with two parameters of generalization. We are

able, in a manner analogous to the classic Mandelbrot set, to use the critical point dynamics to locate Julia sets with visually rich behavior.

Specifically, we consider the complex dynamics of functions of the form

$$f_{\alpha,q}(z) = f(z) = \alpha\left(\tau^z - \bar{\tau}^z\right) \text{ where } \tau = \frac{1+\sqrt{q}}{2} \text{ and } \bar{\tau} = \frac{1-\sqrt{q}}{2}.$$ While the function

depends upon the parameters α and q, we will usually call the function $f(z)$ for

brevity. Of course, the Binet formula occurs when $\alpha = \dfrac{1}{\sqrt{5}}$ and $q = 5$. We will determine

critical points for these functions and create images of the behavior of the critical point relative to the parameter α. These critical point images are an analog of the classic Mandelbrot set [5-10], and like the classic Mandelbrot set, we are able to use these images to identify values of α that give rise to complicated filled in Julia sets for these families of functions. The function $f_{\alpha,q}(z)$ is also related to the exponential

functions αe^z; each of the terms of $f_{\alpha,q}(z)$ corresponds to an exponential function. The

dynamics of αe^z are discussed in [11-12].

2. The Critical Points

Given $f(z) = \alpha\left(\tau^z - \bar{\tau}^z\right)$ we see that $f'(z) = \alpha\left(\tau^z \ln(\tau) - \bar{\tau}^z \ln(\bar{\tau})\right)$. We note that

when $q > 1$, then $\bar{\tau} < 0$ and hence $\ln(\bar{\tau})$ is multi-valued. If we formally solve for the

critical points; that is, solve $f'(z) = 0$ for z, we obtain $z = \dfrac{\ln\left(\dfrac{\ln(\bar{\tau})}{\ln(\tau)}\right)}{\ln(\tau) - \ln(\bar{\tau})}$. Since the

logarithm is multi-valued, there will be many critical points. Nonetheless, we will take $z*$ to be the critical point associated with the principal value for $\ln(\bar{\tau})$ and consider it to be the principal critical point. Notice that the principal critical point depends upon q, but not upon α.

For example, when $q = 5$ the principal critical point is approximately -0.333041+0.702924i. If we consider the iteration of f on the principal critical point for different α, different behaviors occur. For example, when $\alpha = 1$ the iterates quickly become huge, for $\alpha = 0.1$, the iterates are attracted to the fixed point 0, and when $\alpha = 2 + i$, the iterates are attracted to the 4-cycle that is approximately 1.13105+1.60132i, 1.28108+3.63822i, -2.48557+3.31337i, and -0.316386+0.597539i. In the next section we will consider images giving information about these behaviors.

3. Dynamics of the Principal Critical Point

Figure 1 shows the behavior of principal critical point for $q = 5$ as the complex parameter α is varied. The center of the image corresponds to $\alpha = 0.63 + 1.67i$ and the width the image is 4.5. For each α corresponding to a pixel position, if iteration of the critical point becomes large (1e5), then we consider it to have escaped and those points are shown in grayscales, with black being rapid escape and white being slow escape. Color (hue) in the portion that remains bounded specifies periodicity of the cycle to which it is

attracted. For our images we tested for periodicity using the built-in tolerance of the programming language J [13]. It considers floating point numbers equal if the relative difference is less than $2^{-44} \approx 5.6 \times 10^{-15}$ in magnitude. Note that in some cases this could lead to incorrect conclusions. For example, it might be found that a point is seen to be in a 14-cycle within tolerance while if further iteration were done it would be seen that eventually it was in a 7-cycle within tolerance. Thus, we attempt to identify cycle patterns quickly, rather than attempting to see if the cycle structure simplifies on further iteration. We accept these computations as they are designed but remain aware that the periodicities are not examined carefully, simply mechanically with the tolerance scheme we have described. We do typically use one further exception: if the real or imaginary parts are less than the tolerance, $2^{-44} \approx 5.6 \times 10^{-15}$, in magnitude, then we consider that part of the complex number to be exactly zero. Using these convergence requirements, only one tenth of one percent of the pixels in Figure 1 correspond to values for which the behavior was not determined after 32768 iterations. Notice that there are features reminiscent of the ordinary Mandelbrot set, such as sequences of buds, and yet there are quite a few features that are dramatically different. For example the distorted cyan region at the top or the green bud on the left that has a large side bud.

The large blue portion of Figure 1 corresponds to primarily to points α attracted to a fixed point although that fixed point depends on α. The blue points in the lower circular region are attracted to the fixed point 0. Note that while this image highlights the primary component of the bounded region, many other smaller components appear in the image and many others appear outside the region shown by the image. In particular, more regions appear if we expand the domain of the image. Such an image with width 22 is shown at [14] and the structure in Figure 1 along with two smaller sets resembling the classic Mandelbrot set may be seen.

The coloring scheme in Figure 1 is such that grayscales show escape time and periodicity of iteration of the critical point is shown by hues, using the following correspondence: 1-cycles are in blue, 2-cycles are in green, 3-cycles are in cyan, 4-cycles are in red, 5-cycles are in yellow, 6-cycles are in orange, 7-cycles are in light green, 8-cycles are in light blue, 9-cycles are in red-magenta, 10-cycles are in green-blue, 11-cycles are in purple, 12-cycles are in magenta, and then colors are recycled modulo 12 so that 13-cycles would be shown in blue, the same color as 1-cycles. Lighter color shades are used when convergence is rapid and darker shades are used when the convergence was slow. That convention is the opposite of what we use for the grayscales so that there is good contrast at the boundary between those regions.

When $q = 15$, the critical point is approximately -0.38474+0.46808i. Figure 2 shows the behavior of the critical point using the same coloring scheme as was used for Figure 1. Again, position in the image corresponds to α. In Figure 2, the image is centered on $\alpha = 0.3 + 1.1i$ and the image has a width of 3.6. The figure is more symmetric than Figure 1 but the cyan bud is still highly distorted.

When $q = 610$ the principal critical point is approximately -0.283905+0.150034i. Figure 3 shows the behavior of the critical point in that case; the image is centered at 1.51i and has width 4.44. The basins that remain bounded now form a much more symmetric figure. The upper portion is similar to the ordinary Mandelbrot set, but there is substantially more structure that exists beneath it. In general, as q increases, the primary

bounded basins appear to become more symmetric. A few dozen further examples and zooms into details may be seen at [14].

Figure 4 shows a zoom into the region between the lower blue circular bulb in Figure 2, just above the green bulb; the center is -0.15-0.12i and the width is 0.39. However, for this image we used tolerance in cycle checking, but did not force complex parts less than tolerance in magnitude to be zero. Thus we see that there is a great deal of ghosting by numeric cycles very close to zero within the basin associated with the fixed point at 0.

4. Julia Sets

Filled in Julia sets are created by taking a fixed function and considering the escape/convergence time for initial points that correspond to screen position. Here, we fix α and q in order to get a specific function to iterate. In Figure 5 we show the escape and/or convergence time for the filled in Julia set associated with $\alpha = -1.03038 + 1.68012i$ and $q = 5$ that comes from a distorted green bud seen on the left of Figure 1. Here the window is centered at -9.4+9i with a width of 14. The green region corresponds to regions with a period 2 attractor and purple corresponds to period one. Points corresponding to escape are shown in blue. Notice that the green regions have asymmetric arms. The distortion is expected since α was selected from a distorted bud.

Figure 6 gives the Julia set for $\alpha = -0.240908-0.220664i$ when $q = 610$. The window is centered at -0.8 + 9.5i with a width of 0.3. Here points corresponding to 24-cycles are shown in green, those corresponding to 1-cycles are in purple, and escape is shown in blue. This is a wild, complex Julia set, but no distortion is apparent as would be expected since no glaring distortion is apparent in the critical point escape time image for $q = 610$.

Figure 7 shows a spiral associated with a period one attractor. This arises from $\alpha = -0.0850265 + 0.311764i$ and $q = 610$. The window is centered at -0.076+5.76i and has a width of 1.3248. The period one points correspond to purple arches and escape time corresponds to the hues in the spirals.

Figure 8 shows a spiral associated with a period nine attractor. This arises from $\alpha = -0.202444 + 0.251031i$ and $q = 610$. The window is centered at -0.1288+5.71i and has a width of 1.232. The period one points correspond to purple arches and period 9 points to the red; escape time corresponds to the blue in the spirals.

5. Conclusions

Generalized Binet functions have a principal critical point that allows for critical point escape time images to be created that, like the classic Mandelbrot set, are a guide to visually dramatic Julia sets. We have seen that for low values of q, images of the critical point dynamics show distortion that carries over to the corresponding Julia sets. For larger values of q, the critical point dynamics show much more symmetry, but remain more complicated than the classic Mandelbrot set. In all cases we are able to use the critical point dynamic images as a guide into filled Julia set images with rich, beautiful behavior.

References

[1] Hoggatt, VE. Jr. Fibonacci and Lucas Numbers. Santa Clara: The Fibonacci Association; 1979.

[2] Rosen KH. Elementary Number Theory and its Applications, 4th edition. Reading: Addison-Wesley; 1999.

[3] Strayer JK. Elementary Number Theory. Boston: PWS Publishing; 1993.

[4] Reiter CA. Views of Fibonacci dynamics. Computers & Graphics 2004;28:297-300. Auxiliary web material: http://www.lafayette.edu/~reiterc/mvp/fib_v/index.html.

[5] Chen N, Zhu XL Chung KW. M and J sets from Newton's transformation of the transcendental mapping $F(z) = e^{z^w + c}$ with vcps. Computers & Graphics 2002;26:371-383.

[6] Chung KW, Chan HSY, Chen N. General Mandelbrot sets and Julia sets with color symmetry from equivariant mappings of the modular group. Computers & Graphics 200;24:911-918.

[7] Devaney R. Chaos, Fractals and Dynamics, Computer Experiments in Mathematics. Menlo Park: Addison-Wesley; 1990.

[8] Mandlebrot BB. The Fractal Geometry of Nature. New York: W. H. Freeman and Company; 1982.

[9] Peitgen H-O, Jürgens H, Saupe D. Chaos and Fractals, New Frontiers of Science. New York: Springer-Verlag; 1992.

[10] Peitgen H-O, Richter PH. The Beauty of Fractals. Berlin: Springer-Verlag; 1986.

[11] Devaney R. Julia sets and bifurcation diagrams for exponential maps. Bulletin of the American Mathematic Society 1984;11:167-171.

[12] Romera M, Pastor G, Alvarez G, Montoya M. Growth in complex exponential dynamics. Computers & Graphics 2000;24:115-131.

[13] Jsoftware, http://www.jsoftware.com.

[14] Chen N, Reiter CA, Auxiliary materials for Generalized Binet Dynamics, http://www.lafayette.edu/~reiterc/mvq/gbd/index.html; 2005.
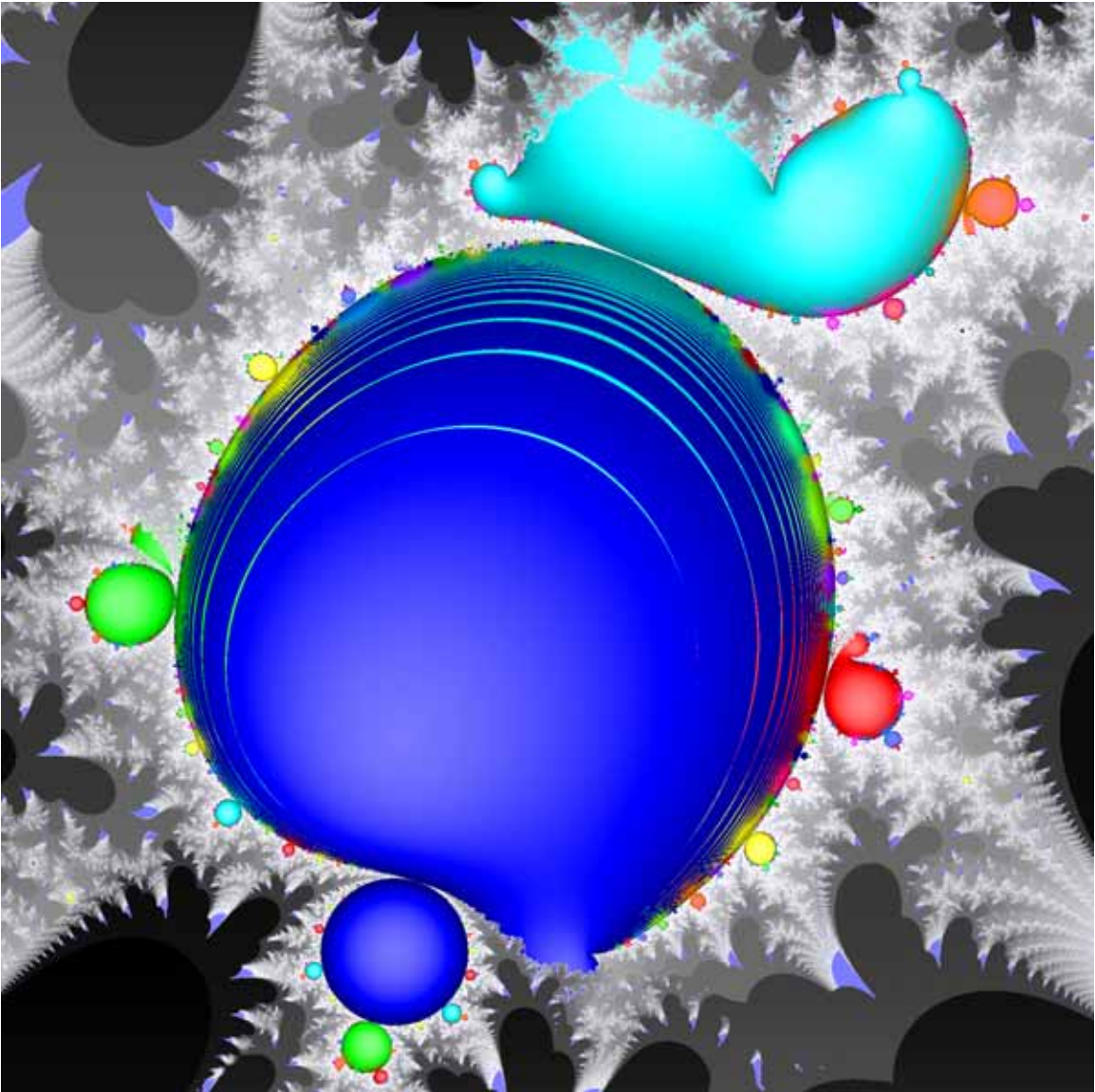
Figure 1. Parameter space behavior of the critical point when *q*=5. The center is $0.63 + 1.67i$ and the width is 4.5.
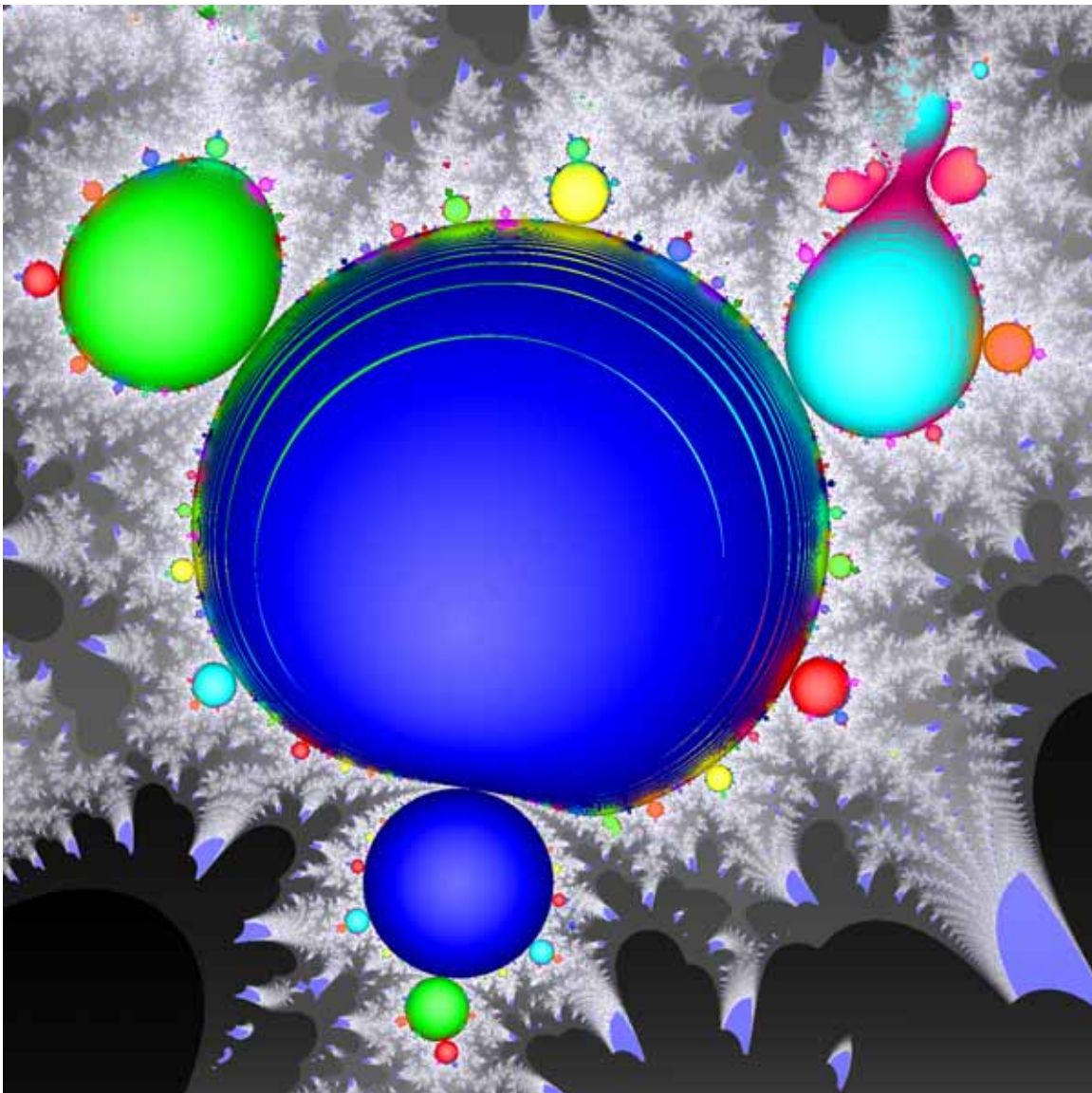
Figure 2. Parameter space behavior of the critical point when q=15. The center is $0.3+1.1i$ and the width is 3.6.
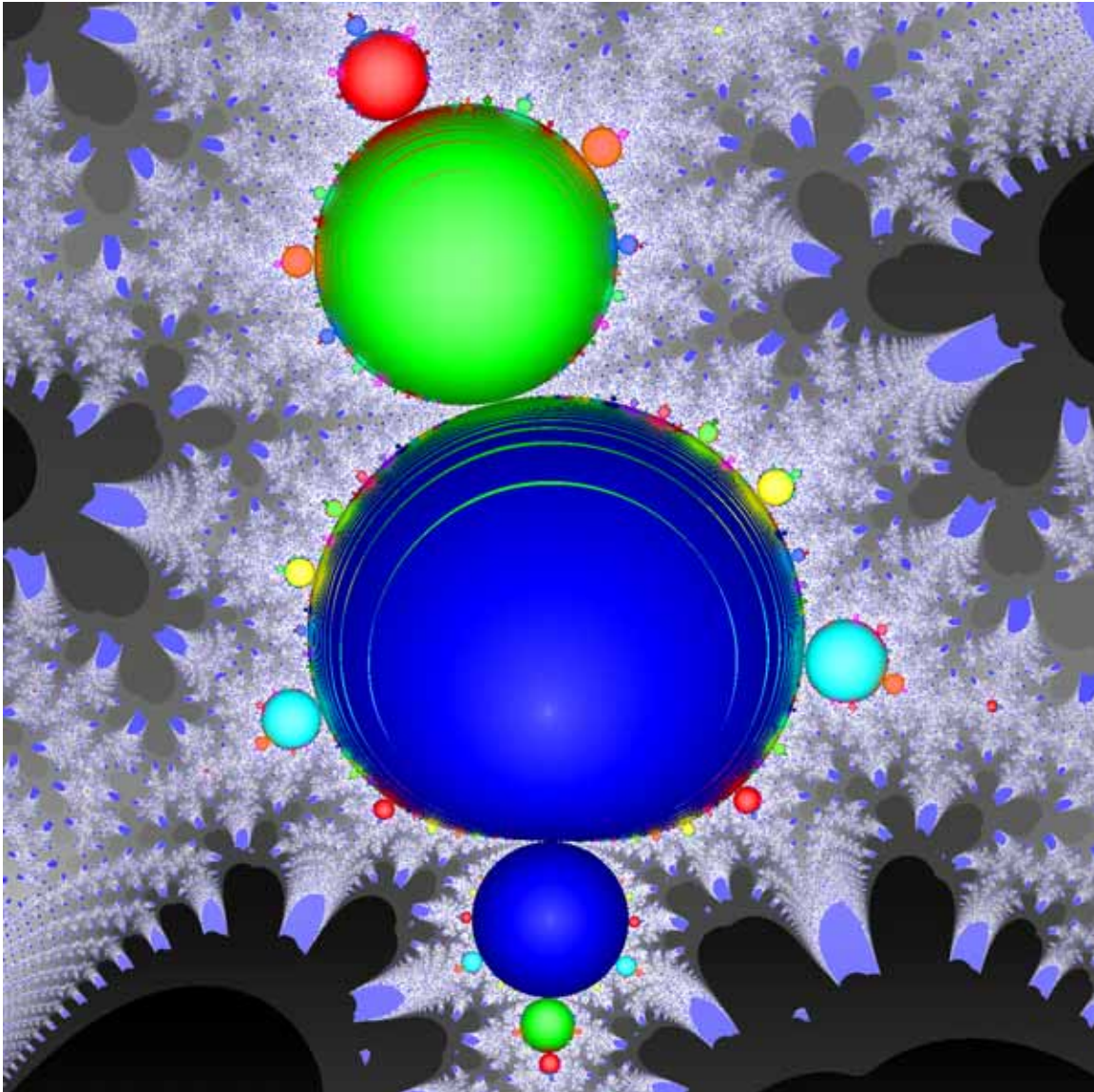
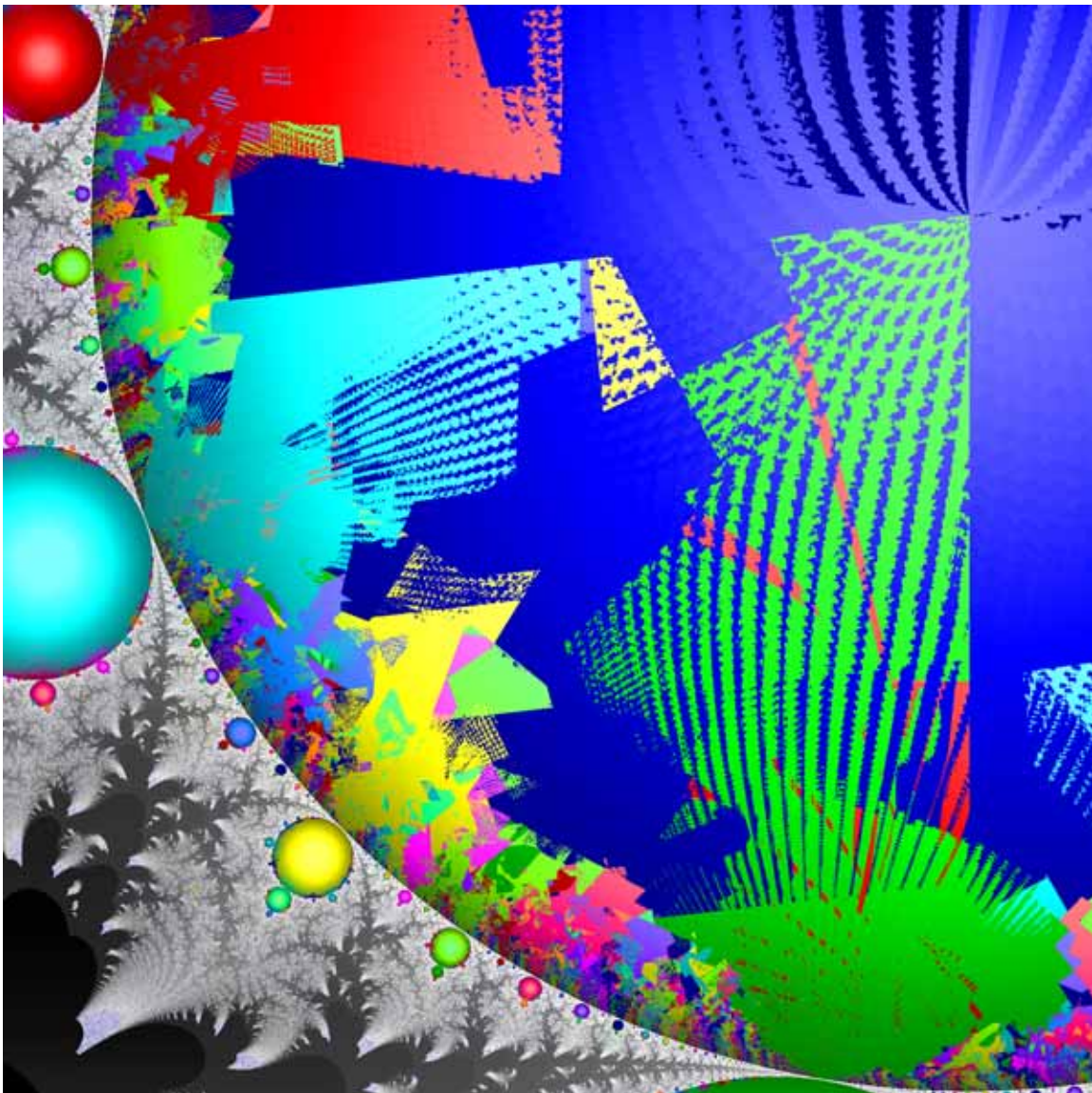Figure 3. Parameter space behavior of the critical point when q=610. The center is $1.51i$ and the width is 4.44.

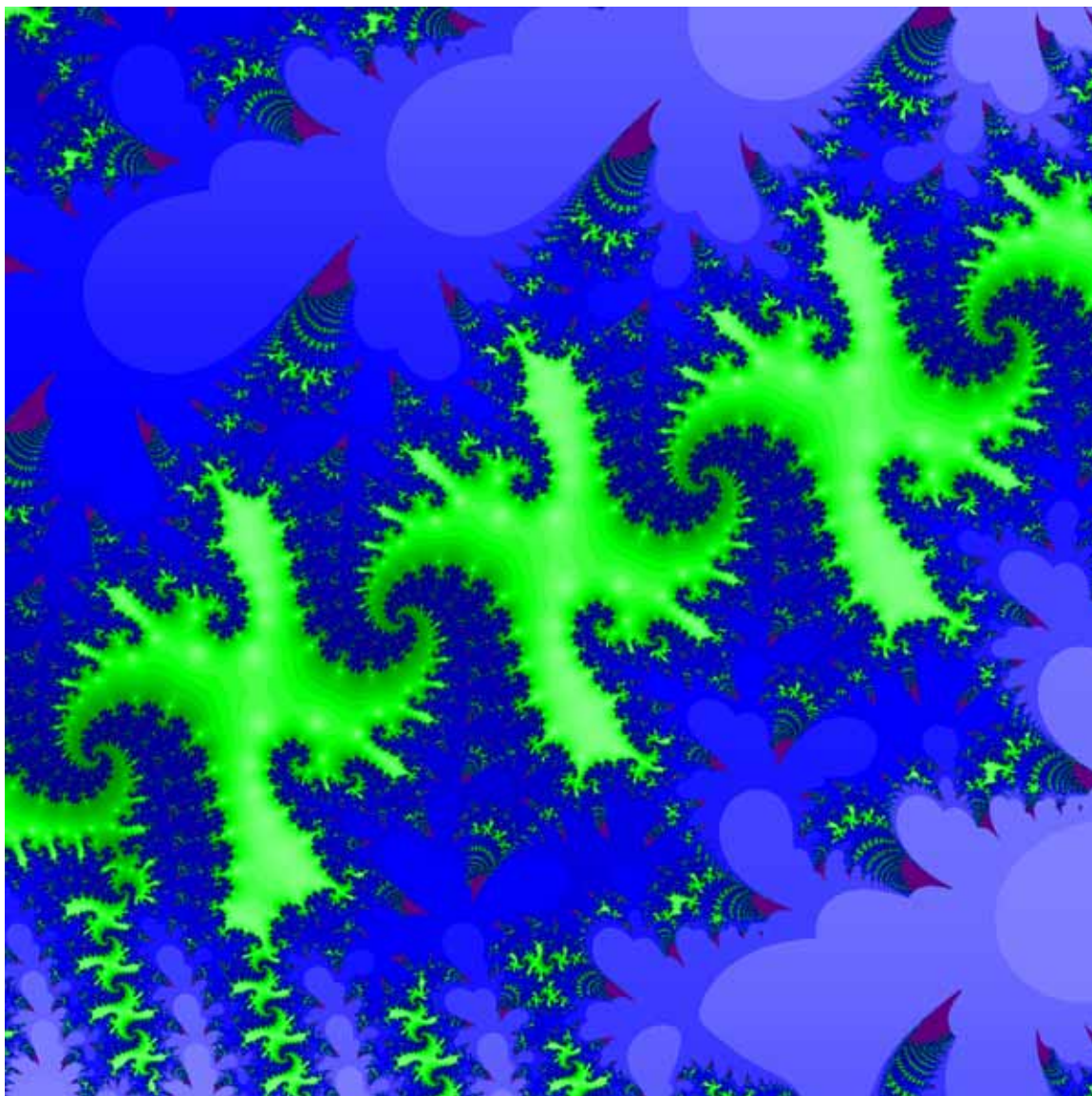Figure 4. Parameter space zoom for *q*=15 with no fuzz removal. The center is -0.15-0.12i and the width is 0.39.

Figure 5. A Julia set from a distorted $q = 5$ bud. The center is -9.4+9i and the width is 14.
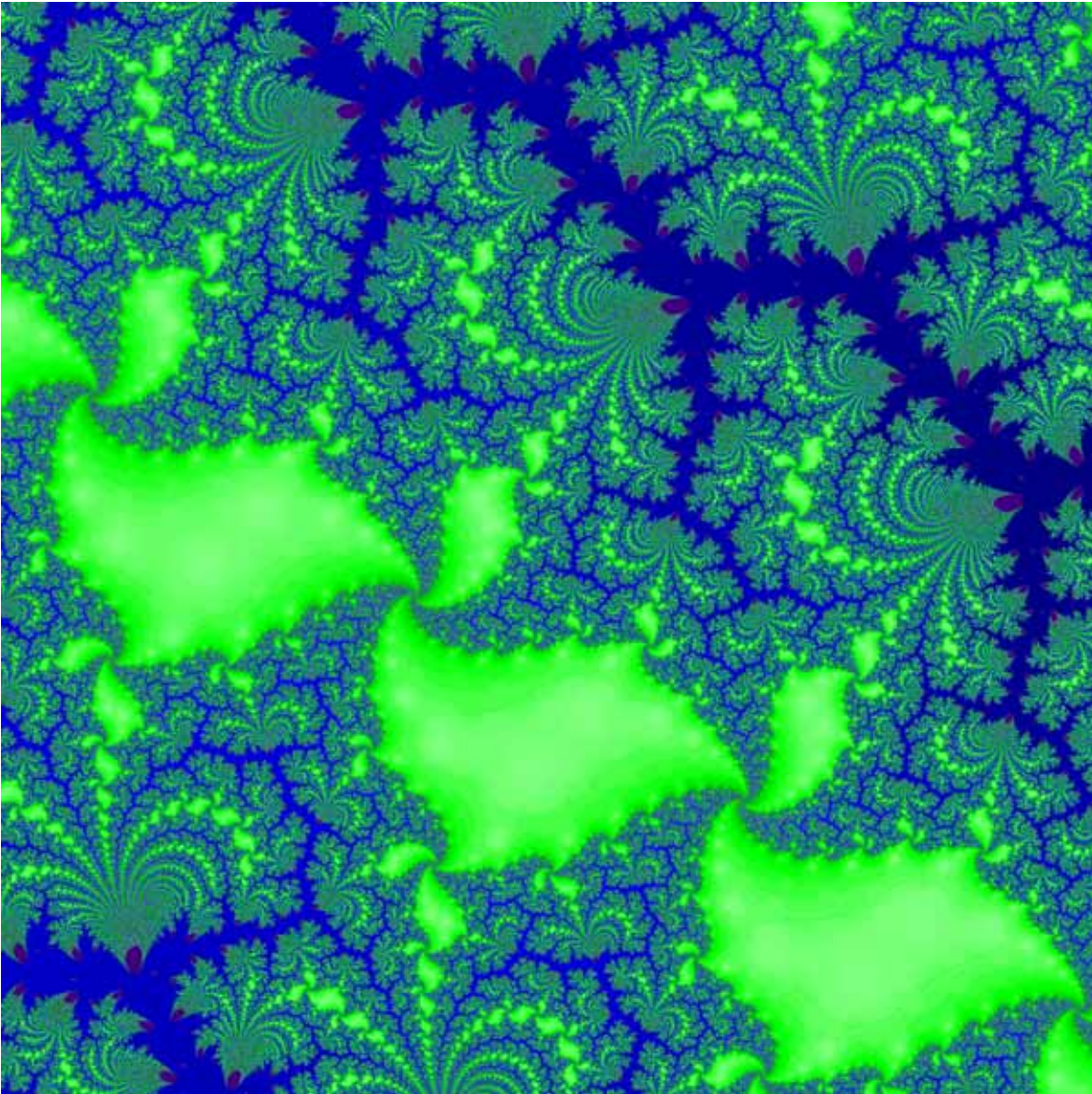
Figure 6. A $q = 610$ Julia set with period 24 attractors. The center is -0.8 + 9.5i and the width is 0.3.

Figure 7. A $q = 610$ Julia set spiral with period 1 attractors. The center is -0.076+5.76i and the width is 1.3248.
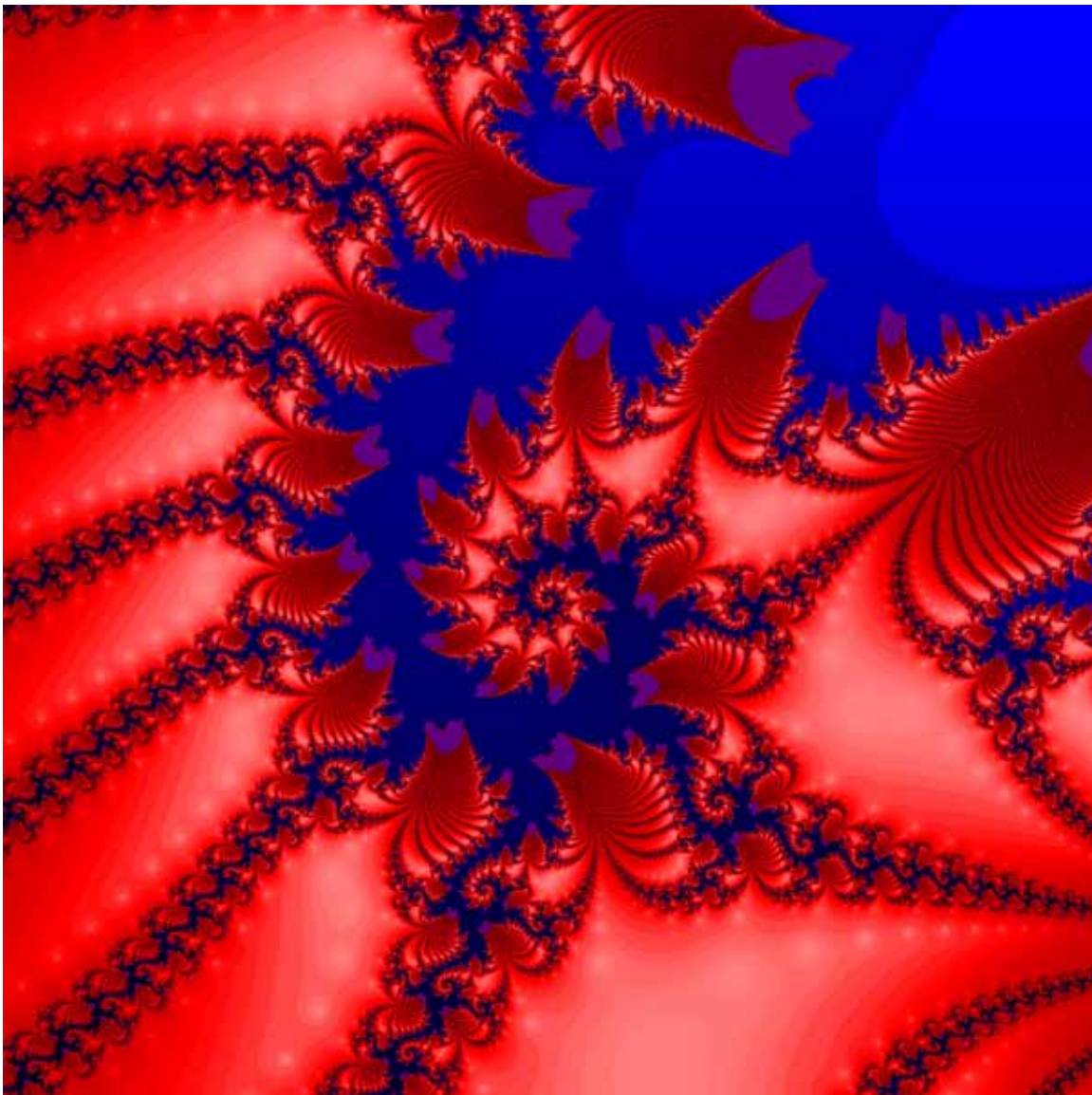
Figure 8. A $q = 610$ Julia set spiral with period 9 attractors. The center is -0.1288+5.71i and the width is 1.232.